Cancer Letters 465 (2019) 68–81

Contents lists available at ScienceDirect

Cancer Letters

journal homepage: www.elsevier.com/locate/canlet

Original Articles

Phloridzin docosahexaenoate, a novel fatty acid ester of a plant polyphenol, inhibits mammary carcinoma cell metastasis

Wasundara Fernando[a], Krysta Coyle[a], Paola Marcato[a,b], H.P. Vasantha Rupasinghe[a,d], David W. Hoskin[a,b,c,*]

[a] Department of Pathology, Faculty of Medicine, Dalhousie University, Halifax, NS, Canada
[b] Department of Microbiology and Immunology, Faculty of Medicine, Dalhousie University, Halifax, NS, Canada
[c] Department of Surgery, Faculty of Medicine, Dalhousie University, Halifax, NS, Canada
[d] Department of Plant, Food and Environmental Sciences, Faculty of Agriculture, Dalhousie University, Truro, NS, Canada

ARTICLE INFO

Keywords:
Flavonoid
Breast cancer
Migration
Invasion
Metastasis

ABSTRACT

Triple-negative breast cancer (TNBC) tends to recur and metastasize following initial chemotherapy, which presents a treatment challenge. Here, we detail the anti-metastatic activity of phloridzin docosahexaenoate (PZ-DHA), synthesized from the natural polyphenol, phloridzin, and the ω-3 fatty acid, docosahexaenoic acid. Sub-cytotoxic PZ-DHA suppressed the migration of MDA-MB-231, SUM149, and 4T1 cells, as well as invasion by MDA-MB-231 and 4T1 cells. Sub-cytotoxic PZ-DHA also inhibited MDA-MB-231 expression of matrix metalloproteinase 2, and expression of epithelial-to-mesenchymal transition-associated transcription factors by MDA-MB-231 and SUM149 cells. Transforming growth factor-β-induced Rho GTPase signaling in MDA-MB-231 cells and non-malignant MCF-10A mammary epithelial cells was suppressed by sub-cytotoxic PZ-DHA, which also inhibited Akt/phosphoinositide 3-kinase and extracellular signal-regulated kinase 1 and 2 signaling in MDA-MB-231 cells. Finally, intraperitoneal administration of PZ-DHA suppressed the metastasis of 4T1 and GFP-transfected MDA-MB-231 cells from the mammary fat pad to the lungs of BALB/c and NOD-SCID female mice, respectively, which was unrelated to any inhibition of primary tumor growth. There was no evidence of toxicity as PZ-DHA treatment did not affect liver or kidney function. We conclude that PZ-DHA might prevent or inhibit the progression of TNBC.

1. Introduction

Triple-negative breast cancer (TNBC) is associated with tumor recurrence, metastasis and poor clinical prognosis; therefore, this disease remains a major cause of cancer-related deaths among women worldwide [1]. TNBC cells lack estrogen receptors or human epidermal growth factor receptor 2, and are thus refractory to targeted breast cancer therapies, leading to a demand for novel drugs to treat the disease more effectively with minimal adverse side effects. The metastatic cascade of TNBC and other breast cancers consists of growth, migration, invasion and establishment of micrometastases by disseminated tumor cells at a distant site [2]. Hematogenic or lymphogenic spread of neoplastic cells from a primary breast tumor leads to the establishment of secondary metastatic lesions; preferentially, in bones, lungs, liver and/or brain [3,4]. Aberrant activation of signaling pathways including those that involve Akt/phosphatidylinositol 3-kinase (PI3K), mitogen-activated protein kinases (MAPK) and small molecular Rho GTPase, promotes survival and migration of breast cancer cells [5–7]. Rho GTPase signaling-induced cytoskeletal changes, together with activation of the epithelial-to-mesenchymal transition (EMT), leads to the acquisition of a mesenchymal-like phenotype by breast cancer cells [8]. The accompanying loss of epithelial characteristics is associated with decreased expression of epithelial-like markers such as E-cadherin. The subsequent dissemination of breast cancer cells from a primary tumor involves transforming growth factor (TGF)-β, which is a potent stimulator of cell migration [9–12]. The metastatic spread of breast cancer cells is also dependent on the degradation of extracellular matrix (ECM) proteins by matrix metalloproteinases (MMPs), which facilitates tumor cell intravasation and extravasation [2].

Plant polyphenols are a group of naturally-occurring phytochemicals that possess anti-proliferative and anti-metastatic activities against breast cancer cells [13–15]. Flavonoids, a sub-group of plant polyphenols possess a wide-range of disease-fighting properties, including anti-cancer activities [16–19]. Flavonoids that inhibit breast cancer cell

* Corresponding author. Department of Pathology, Faculty of Medicine, Dalhousie University, Halifax, NS, Canada.
E-mail address: d.w.hoskin@dal.ca (D.W. Hoskin).

https://doi.org/10.1016/j.canlet.2019.08.015
Received 22 May 2019; Received in revised form 17 August 2019; Accepted 26 August 2019

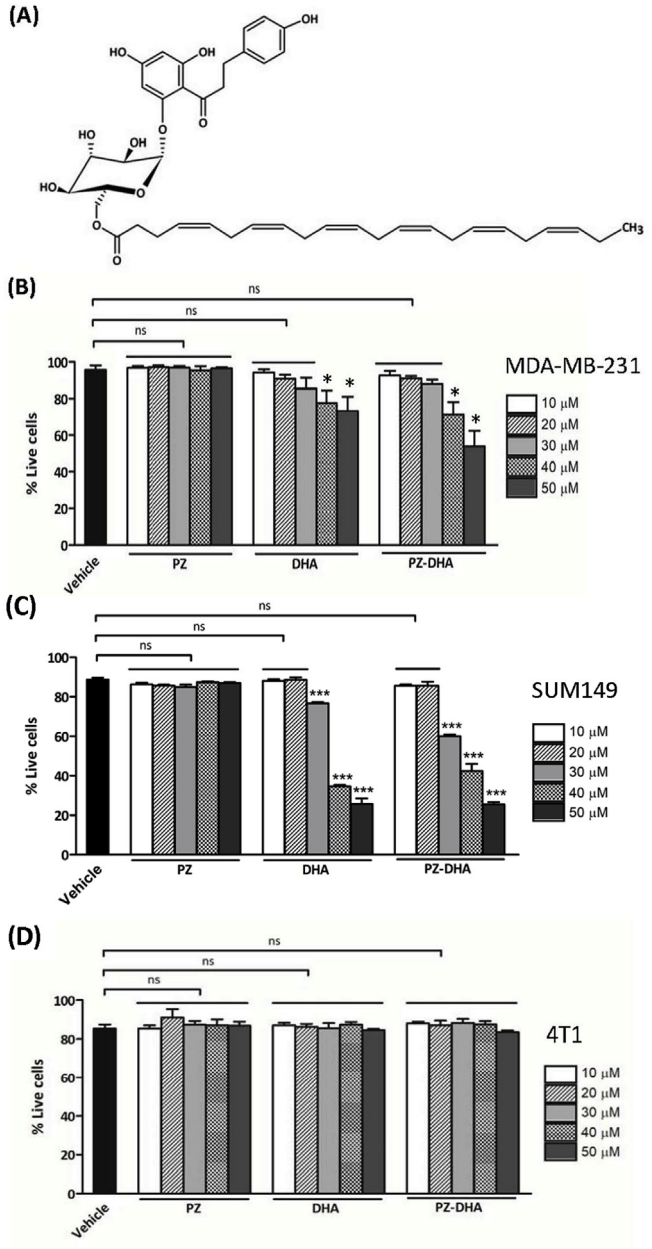

Fig. 1. Structure of PZ-DHA and its concentration-dependent impact on mammary carcinoma cell viability. **(A)** Chemical structure of PZ-DHA. **(B)** MDA-MB-231, **(C)** SUM149, or **(D)** 4T1 mammary carcinoma cells were treated with the indicated concentrations of PZ, DHA, PZ-DHA or the vehicle alone, cultured for 72 h and stained with 7-AAD for analysis by flow cytometry. Percentage of dead cells was determined and data expressed as mean ± SEM of 3 independent experiments. Differences between the means were compared by ANOVA and Tukey's multiple comparisons test; ns: not significant, *P < 0.05.

invasion and metastasis are of particular interest [20–22]. However, the clinical application of flavonoids is restricted by their poor cellular uptake and bioavailability; therefore, attempts have been made to synthesize flavonoid derivatives that are free of these limitations. For example, novel flavonoids derived from myricetin exert *in vitro* and preclinical anti-cancer activity through mitochondrial targeted-redox active mechanisms [23]. VI-14, another novel flavonoid derivative, interferes with migration and invasion of MDA-MB-231 and MDA-MB-435 breast cancer cells by inhibiting ECM degradation-associated proteins [24]. A series of flavone analogs that selectively bind to eukaryotic elongation factor 2A of breast cancer cells exert imidazole ring-independent anti-proliferative activity [25].

Phloridzin docosahexaenoate (PZ-DHA; see Fig. 1A for structure) combines, via an acylation reaction, phloridzin (PZ), a flavonoid precursor that is abundant in apple peels, and docosahexaenoic acid (DHA), an ω-3-fatty acid, in order to improve stability of DHA and cellular uptake of PZ [26]. Earlier studies have established that PZ-DHA inhibits the *in vitro* growth of human hepatocellular carcinoma (HepG2), acute monocytic leukemia (THP1), chronic myelogenous leukemia (K562) and acute T cell leukemia (Jurkat) cells [27,28], as well as suppressing lipopolysaccharide-induced pro-inflammatory responses by THP-1 macrophages [29]. In addition, we previously reported that PZ-DHA exerts selective cytotoxic activity against mammary carcinoma cells (MDA-MB-231, MDA-MB-468, 4T1, MCF-7 and T-47D) in comparison to non-malignant cells (human mammary epithelial cells, MCF-10A and human dermal fibroblasts), as well as inhibiting the growth of MDA-MB-231 tumor xenografts in non-obese diabetic severe combined-immunodeficient (NOD-SCID) mice [30]. In the current study, we explored the anti-metastatic activity of PZ-DHA and, for the first time, show that sub-cytotoxic PZ-DHA interfered with metastasis-associated signaling pathways and suppressed the migration, invasion and epithelial-to-mesenchymal transition of TNBC cells, as well as reducing lung metastases in 2 different mouse models of metastatic TNBC.

2. Materials and methods

2.1. Reagents and chemicals

Dulbecco's Modified Eagle's Medium (DMEM), F12/DMEM, F12 medium, fetal bovine serum (FBS), horse serum, N-2-hydroxyethylpiperazine-N′-2-ethanesulfonic acid (HEPES), L-glutamine, penicillin–streptomycin, trypsin (0.25% with 1 × EDTA), TryPLE Express, and fibronectin were purchased from Life Technologies Inc. (Burlington, ON). DHA and 7-aminoactinomycin (7-AAD) cell viability staining solution was purchased from Nu-Chek Prep Inc. (Elysian, MN) and eBioscience Inc. (San Diego, CA), respectively. Human epidermal growth factor (EGF), and TGF-β were purchased from PeproTech (Rocky Hill, NJ). PZ, bovine insulin, human insulin, hydrocortisone, mitomycin C, gelatin, 6-thioguanine, puromycin, and dimethyl sulfoxide (DMSO) were purchased from Sigma-Aldrich Canada (Oakville, ON). Matrigel was obtained from Corning Life Sciences (Tewkbury, MA). Diff-Quik staining kit was purchased from Siemens Healthcare Diagnostics (Los Angeles, CA). Rodent M block, mouse-on-mouse horse radish peroxidase (HRP)-polymer, MACH 4 MR AP polymer and Vulcan Fast red chromogen kit were purchased from Biocare Medical (Markham, ON) and the HRP/DAB detection system was obtained from Agilent Technologies (Mississauga, ON).

2.2. Antibodies

Anti-phospho-phosphatase and tensin homolog (PTEN; Ser380), anti-phospho-phosphoinositide-dependent kinase 1 (PDK1; Ser241), anti-phospho-mammalian target of rapamycin (mTOR, Ser2448), anti-phospho-glycogen synthase kinase 3β (GSK3β, Ser9), anti-phospho-c-RAF (Ser259), anti-phospho-p44 (ERK1, Thr202)/p42 (ERK2,Tyr204), anti-PTEN, antil-PDK1, anti-mTOR, anti-GSK3β, anti-c-RAF, anti-p44/p42, anti-TCF8/ZEB-1, anti-β-catenin, anti-Slug-1, anti-vimentin, anti-pan-cadherin, anti-RhoA, anti-Cdc42, anti-Rac1/2/3, anti-α-tubulin, HRP-conjugated rabbit anti-actin, HRP-conjugated donkey anti-rabbit and goat anti-mouse IgG antibodies (Ab) were purchased from Cell Signaling Technology Inc. (Danvers, MA). Anti-Ki67, anti-MMP-2 and anti-CD31 Abs were purchased from Abcam Inc. (Toronto, ON). Anti-phospho-GSK3β (Tyr216) Ab was purchased from Sigma Aldrich Canada.

2.3. Cell culture

MDA-MB-231 cells were from Dr. S. Drover (Memorial University of

Newfoundland, St. John's, NL). 4T1 mouse mammary carcinoma cells were from Dr. D. Waisman (Dalhousie University, Halifax, NS). SUM149 cells were from the American Type Culture Collection (ATCC; Manassas, VA). Mammary carcinoma cell lines were authenticated by short tandem repeat analysis conducted by ATCC and DDC Medical DNA Diagnostic Center (Fairfield, OH). MDA-MB-231 and 4T1 mammary carcinoma cells were maintained in DMEM supplemented with 10% v/v heat-inactivated FBS, 5 mM HEPES (pH 7.4), 2 mM L-glutamine, 100 U/ml penicillin and 100 μg/ml streptomycin (complete DMEM). GFP-transfected MDA-MB-231 cells were maintained in complete DMEM plus 0.25 μg/ml puromycin. SUM149 cells were grown in F-12 medium supplemented with 5% v/v heat-inactivated FBS, 5 mM HEPES, 5 μg/ml human insulin, and 0.05 μg/ml hydrocortisone. MCF-10A cells were purchased from ATCC and grown in F12/DMEM (1:1) supplemented with 10% horse serum, 0.02 μg/ml EGF, 0.05 μg/ml hydrocortisone, 10 μg/ml bovine insulin, 100 U/ml penicillin and 100 μg/ml streptomycin. Cell lines were maintained at 37 °C in a humidified 10% (MDA-MB-231 and 4T1 cells) or a 5% (SUM149 and MCF-10A cells) CO_2 atmosphere.

2.4. 7-AAD staining

Cytotoxicity was measured by 7-AAD staining of MDA-MB-231, SUM149, and 4T1 cells following culture for 72 h in the absence or presence of the indicated concentrations of PZ, DHA, or PZ-DHA. Cells were harvested and treated with 5 μl 7-AAD solution (eBioscience Inc. San Diego, CA, USA) at room temperature for 5 min. Cells were then washed and analyzed using a FACSCalibur flow cytometer (BD Bioscience, Mississauga, ON).

2.5. Gap-closure assays

MDA-MB-231 (10,000 cells in 100 μl), SUM149 (10,000 cells in 100 μl) or 4T1 (8000 cells in 100 μl) cells were seeded into 2-well culture inserts and cultured overnight. Adherent cells were treated with 10 μg/ml (MDA-MB-231, SUM149) or 20 μg/ml (4T1) of mitomycin C in serum-free medium for 2 h at 37 °C. Cells were allowed to recover for 12 h in complete medium and then cultured in the absence or presence of 10 μM PZ, DHA, or PZ-DHA for 24 h. Culture inserts were removed and the gaps were photographed to establish a baseline, then periodically photographed until the gap was closed in control cultures.

2.6. Trans-well cell migration and chemo-invasion assays

MDA-MB-231, SUM149 or 4T1 cells were cultured for 24 h in the absence or presence of 20 μM PZ, DHA, or PZ-DHA. In other experiments, MDA-MB-231 or MCF-10A cells were pretreated with or without TGF-β (10 ng/ml followed by 5 ng/ml) and then cultured for 24 h (migration) or 72 h (TGF-β-induced migration) in the absence or presence of 20 μM PZ, DHA, or PZ-DHA. Cells were then serum-starved for 6 h (MDA-MB-231, SUM149, 4T1) or 12 h (MCF-10A) and harvested. Aliquots of 5×10^4 cells in 50 μl serum-free DMEM were placed into wells of the upper chamber of the trans-well cell migration apparatus. Bottom chamber wells contained DMEM plus 10% FBS. Migration of cells through an 8 μm porous membrane coated with or without ECM proteins was detected by Diff-Quik staining of the membrane followed by imaging under a light microscope.

2.7. Western blot analysis

MDA-MB-231, SUM149, or MCF-10A cells were cultured for 72 h in the absence or presence of 20 μM PZ, DHA, or PZ-DHA. Cells were then harvested and incubated in ice-cold lysis buffer (50 mM Tris at pH 7.5, 150 mM NaCl, 50 mM Na_2HPO_4, 0.25% sodium deoxycholate (w/v), 0.1% Nonidet P-40 (v/v), 5 mM ethylenediaminetetraacetic acid and 5 mM EGTA) containing freshly added protease inhibitors (1 mM phenylmethylsulfonylfluoride, 10 μg/ml aprotinin, 5 μg/ml leupeptin, 10 μM phenylarsine oxide, 1 mM dithiothreitol and 5 μg/ml pepstatin) in 100 μM Na_3VO_4, 10 mM NaF for 15 min. Protein-rich cell lysates were separated by centrifugation at 14,000 g for 10 min at 4 °C and total protein concentration was determined by Bradford protein assay. Equal amounts protein in denaturing buffer were loaded onto 7.5, 10, 12 or 15% SDS-polyacrylamide gels and electrophoresed. Proteins were transferred to nitrocellulose membranes and blots were blocked for 1 h with 5% non-fat milk or bovine serum albumin in Tween-TBS (250 mM Tris at pH 7.5, 150 mM NaCl and 0.2% Tween-20). Blots were probed overnight at 4 °C with the indicated primary Abs at the supplier-recommended concentrations, then blots were washed thoroughly with Tween-TBS and probed with the appropriate HRP-conjugated secondary Ab for 1 h at room temperature. Even protein loading was confirmed by probing the blots with HRP-conjugated anti-actin Ab or primary Ab against α-tubulin followed with HRP-conjugated secondary Ab. Protein bands were visualized using a ChemidocTouch™ imaging system (Bio-Rad Laboratories, Mississauga, ON).

2.8. Mouse models of metastasis

Six-to-eight-week old BALB/c and NOD-SCID female mice were purchased from Charles River (Lasalle, QC). BALB/c mice were fed a regular rodent diet and water supplied *ad libitum*. NOD-SCID mice were housed under sterile conditions, fed a sterile rodent diet and sterile water supplied *ad libitum*. Mammary carcinoma cells were confirmed to be free of mycoplasma contamination the day before implantation into mice. As depicted in Supplementary Fig. 1A, 4T1 cells (1×10^5) in 50 μl sterile PBS were implanted into the left inguinal mammary fat pad of BALB/c mice (designated day 0). On day 8, mice were randomly assigned into two groups and saline or PZ-DHA (100 mg/kg body weight) was administered by intraperitoneal injection every second day for 9 days. Mice were euthanized on day 17. Primary tumors were fixed in 10% (v/v) acetate-buffered formalin. Lungs were harvested and homogenized in digestion buffer. The resulting cell homogenate was cultured for 14 days in complete DMEM supplemented with 60 μM 6-thioguanine, after which 4T1 colonies were visualized by staining with 0.4% (w/v) crystal violet. GFP-MDA-MB-231 cells were generated as follows. pGipZ-EGFP lentivirus was assembled in HEK293T cells using a second-generation packaging system (pMD2.G, pSPAX2). Lentiviral supernatants were collected and filtered (0.45 μm) prior to being applied to MDA-MB-231 cells, which were then cultured in the presence of lentiviral supernatant for 4 h before replacing with complete DMEM. Cells were selected with 1.5 μg/ml puromycin and maintained by culture in the presence of 0.25 μg/ml puromycin. As shown in Supplementary Fig. 1B, GFP-MDA-MB-231 cells (2×10^6) in 50 μl PBS were mixed with 50 μl Matrigel and injected into the left inguinal mammary fat pad of NOD-SCID mice (designated day 0). On day 21, mice were randomly divided into two groups and saline or PZ-DHA (100 mg/kg) was administered by intraperitoneal injection every second day for 39 days. Mice were euthanized on day 60. Lungs were harvested and a single-cell suspension was generated. Erythrocytes were lysed and following a PBS wash, cells were resuspended in PBS containing 0.5% (w/v) bovine serum albumin. GFP-MDA-MB-231 cells in lung cell preparations were detected by flow cytometry. The volume of 4T1 and GFP-MDA-MB-231 tumors was calculated according to the equation, $L \times P^2$, where L is the longest tumor diameter and P is diameter perpendicular to the longest diameter measured using a digital caliper. Ethics approval for animal use was obtained from the Dalhousie University Committee on Laboratory Animals, and was in accordance with Canadian Council on Animal Care guidelines.

2.9. Histology and immunohistochemistry

Formalin-fixed 4T1 and MDA-MB-231 primary tumors were embedded in paraffin and 5 μm thick sections were generated. Tumor

sections were mounted on glass slides and stained with hematoxylin and eosin for detection of tumor necrosis and tumor-associated blood vessels. Immunohistochemistry was performed to detect the expression of Ki67, MMP-2 and CD31.

2.10. Alanine aminotransaminase (ALT) assay

The liver function of PZ-DHA- and saline-treated 8-week-old female BALB/c mice was assessed using a kit to measure serum ALT (Cayman Chemical, Ann Arbor, MI). Crystalline L-alanine and porcine heart ALT were used as the ALT substrate and the ALT positive control, respectively. Both substances were dissolved in assay buffer (100 mM Tris-HCl, 10 mM sodium bicarbonate, 0.1 mM pyridoxal-5-phosphate and 0.01% sodium azide). NADH and LDH dissolved in assay buffer were used as co-factors for the reaction. The assay was performed in a 96-well plate. L-alanine (150 µl), co-factor mixture (20 µl), porcine heart ALT or serum samples (20 µl) were added to wells and the plate was incubated at 37 °C for 15 min. The reaction was initiated by adding 20 µl of 150 mM α-ketoglutarate, and absorbance was measured at 340 nm using an Asys Expert microplate reader (Biochrom Ltd., Cambridge, UK) once every minute over 5 min. The rate of change in absorbance at 340 nm (ΔA_{340}) was determined using a calibration curve ($R^2 = 0.99$), and ALT enzyme activity in serum samples was determined using the formula below, where, ε is the extinction coefficient of NADH.

$$\text{ALT activity}\left(\frac{\text{U}}{\text{ml}}\right) = \frac{\Delta A_{340}/\text{min} \times 0.21\ ml}{\varepsilon\ mM^{-1}cm^{-1} \times 0.02\ ml}$$

2.11. Creatinine assay

The kidney function of PZ-DHA- and saline-treated 8-week-old female BALB/c mice was assessed using a kit to measure serum creatinine (Cayman Chemical). A calibration curve ($R^2 = 0.98$)for creatinine was generated using a 0.2 mg/ml creatinine stock made in water. Creatinine standard or serum samples (15 µl) were diluted in 100 µl of reaction buffer (sodium borate, creatinine surfactant, and 1 M sodium hydroxide solution) in a 96-well plate. Timing was begun immediately after adding 1.2% picric acid (100 µl), and absorbance was measured at 492 nm using an Asys Expert microplate reader after 1 min and 7 min. Adjusted ΔOD was determined according to formula below. A creatinine calibration curve was generated and creatinine concentration in serum samples was determined.

$$\Delta OD = A_{492\,(7\ min)} - A_{492\,(1\ min)}$$

2.12. Key resources table

Resource	Source	Identifier
Antibodies		
anti- phospho-c-RAF		
anti- Slug-1		
anti-a-tubulin, HRP-conjugated rabbit anti-actin, HRP-conjugated donkey anti-rabbit		
anti-CD31		
anti-Cdc42		
anti-c-RAF		
anti-GSK3ß		
Anti-Ki67		
anti-MMP-2		
anti-mTOR		
anti-p44 (ERK1)/p42 (ERK2)		
anti-pan-cadherin		
Anti-phospho- GSK3ß		
anti-phospho- phosphoinositide-dependent kinase 1		
anti-phospho-glycogen synthase kinase 3β (GSK3ß, Ser9)		
anti-phospho-mammalian target of rapamycin		
Anti-phospho-PTEN		
anti-PTEN		
anti-Rac1/2/3		
anti-RhoA		
anti-ß-catenin		
anti-TCF8/ZEB-1		
anti-vimentin		
goat anti-mouse IgG		
HRP-conjugated anti-actin		
Cell line		
4T1		
MCF-10A		
MDA-MB-231		
SUM149		
Chemical		
7- aminoactinomycin		
a-ketoglutarate		
creatinine		
crystal violet		
dithiothreitol		
DMSO		
EDTA		
ethylenediaminetetraacetic acid		
HEPES		
hydrocortisone		
L- alanine		
L- glutamine		
leupeptin		
mitomycin C		
N-2-hydroxyethylpiperazine-N′-2-ethanesulfonic acid		
Na_3VO_4		
NADH		
penicillin		
pepstatin		
phenylarsine oxide		
phenylmethylsulfonylfluoride		
picric acid		
puromycin		
sodium azide		
sodium bicarbonate		
sodium deoxycholate		
sodium hydroxide		
streptomycin		
Tris-HCl		
ProteinPeptide		
fibronectin		
protease		
serum albumin		
TBS		

3. Results

3.1. Determination of a sub-cytotoxic concentration of PZ-DHA

Flow cytometric analysis of 7-AAD-stained MDA-MB-231, SUM149, and 4T1 triple-negative mammary carcinoma cells was used to determine sub-cytotoxic concentrations of PZ-DHA for use in subsequent experiments. In line with our earlier findings [30], Fig. 1B shows that 72 h exposure to DHA alone and PZ-DHA, but not PZ alone, at 40 and 50 µM, killed MDA-MB-231 cells. SUM149 cells were slightly more sensitive to DHA and PZ-DHA (Fig. 1C). In contrast, Fig. 1D shows that the viability of 4T1 cells was not affected by PZ, DHA, or PZ-DHA at any of the tested concentrations. We therefore applied sub-cytotoxic concentrations (≤ 20 µM) of PZ, DHA, and PZ-DHA to determine whether these phytochemicals affected the metastatic properties of MDA-MB-231, SUM149, and 4T1 cells in the absence of cytotoxicity.

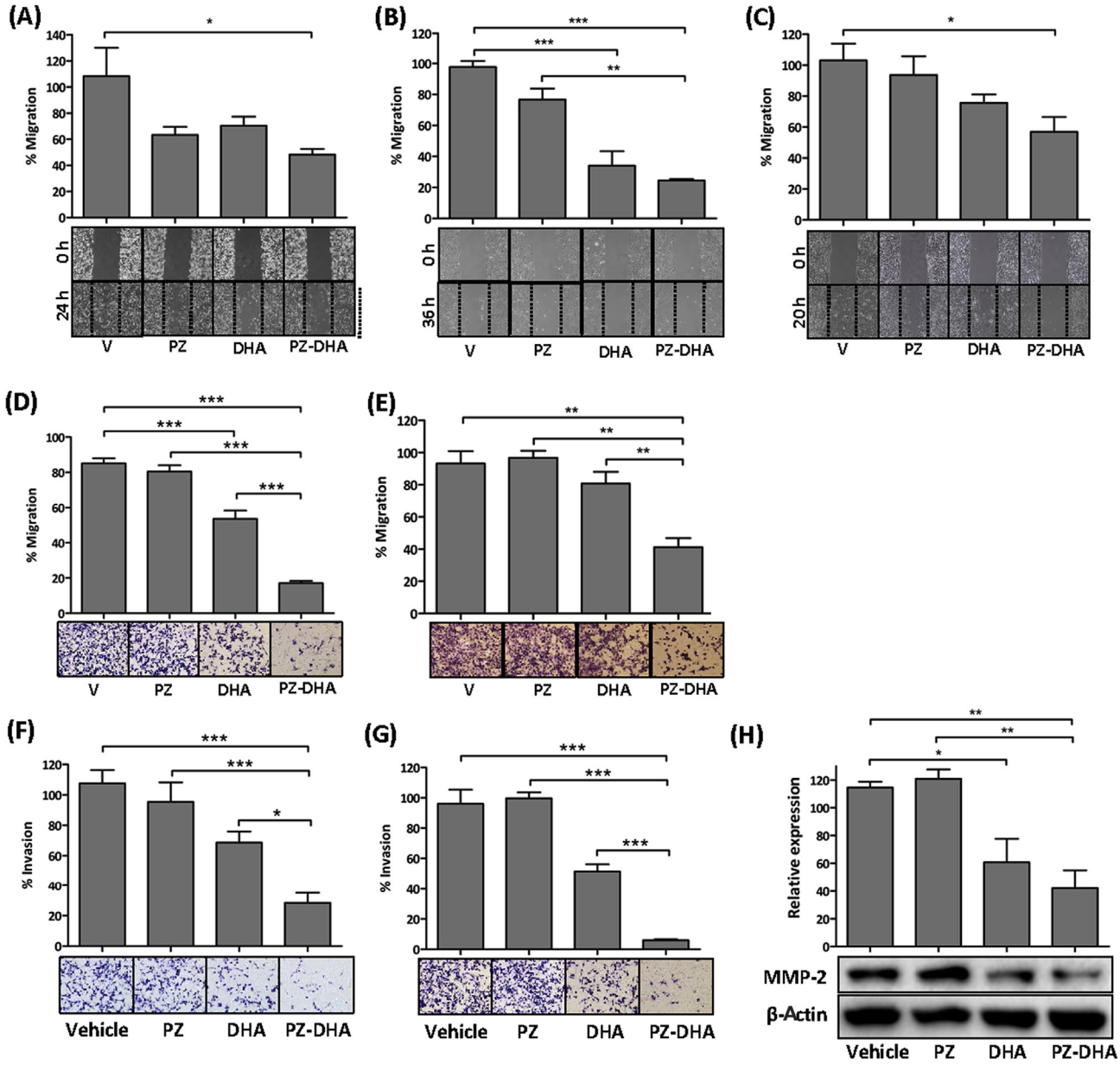

Fig. 2. PZ-DHA inhibits triple-negative mammary carcinoma cell migration and invasion. **(A)** MDA-MB-231, **(B)** SUM149, or **(C)** 4T1 cells were seeded in cell culture inserts and incubated with mitomycin C (MDA-MB-231 and SUM149, 10 μg/ml; 4T1, 20 μg/ml) to prevent proliferation. The cells were treated with PZ, DHA, PZ-DHA (10 μM), vehicle or medium alone for 24 h, then inserts were removed and images were captured until the gap was closed by control cells. Data shown are mean % migration ± SEM of 3 independent experiments. **(D)** MDA-MB-231 and **(E)** SUM149 cells were seeded and treated with PZ, DHA, PZ-DHA (20 μM) or vehicle alone for 24 h, then serum-starved and resuspended in serum-free medium to determine their chemoattractant-induced migration. Images were analyzed using ImageJ software and % migration was calculated. Data shown are mean % migration ± SEM of 3 independent experiments. **(F, G)** MDA-MB-231 cells were seeded and treated with PZ, DHA, PZ-DHA (20 μM) or vehicle alone for 24 h. Treated cells were serum- starved and resuspended in serum-free medium and their chemoattractant-induced migration through membranes coated with **(F)** 10 μg/ml fibronectin or **(G)** 10 μg/ml gelatin was determined. Images were analyzed using ImageJ software and % invasion was calculated. Data shown are representative images and mean % invasion ± SEM of 3 independent experiments. **(H)** MDA-MB-231 cells were treated for 72 h with PZ, DHA, PZ-DHA (20 μM) or vehicle alone. Cells were harvested, lysed and relative expression (± SEM of 3 independent experiments) of MMP-2 was determined by Western blot analysis. Equal protein loading was confirmed by β-actin expression. Differences between the means were compared by ANOVA and Tukey's multiple comparisons test; *P < 0.05, **P < 0.01, and ***P < 0.001.

3.2. PZ-DHA inhibits triple-negative mammary carcinoma cell migration and invasion

A gap-closure assay was used to determine the impact of sub-cytotoxic PZ-DHA on the motility of mammary carcinoma cells. As shown in Fig. 2, sub-cytotoxic PZ-DHA (10 μM) inhibited the migration of triple-negative MDA-MB-231 (Fig. 2A), SUM149 (Figs. 2B), and 4T1 (Fig. 2C) mammary carcinoma cells, as indicated by a reduction in gap closure relative to the untreated control. Treatment with PZ or DHA alone appeared also to reduce migration; however, the effect was not statistically significant with the exception of DHA-treated SUM149 cells. Sub-cytotoxic PZ-DHA had a dramatic inhibitory effect on chemoattractant-induced migration of MDA-MB-231 and SUM149 cells across a transwell membrane (Fig. 2D and E, respectively). DHA alone had a slight but statistically significant inhibitory effect on MDA-MB-231 cells in this assay. Chemoattractant-induced migration of MDA-MB-231 cells across fibronectin-coated (Fig. 2F) and gelatin-coated (Fig. 2G) transwell membranes was also inhibited by sub-cytotoxic PZ-DHA.

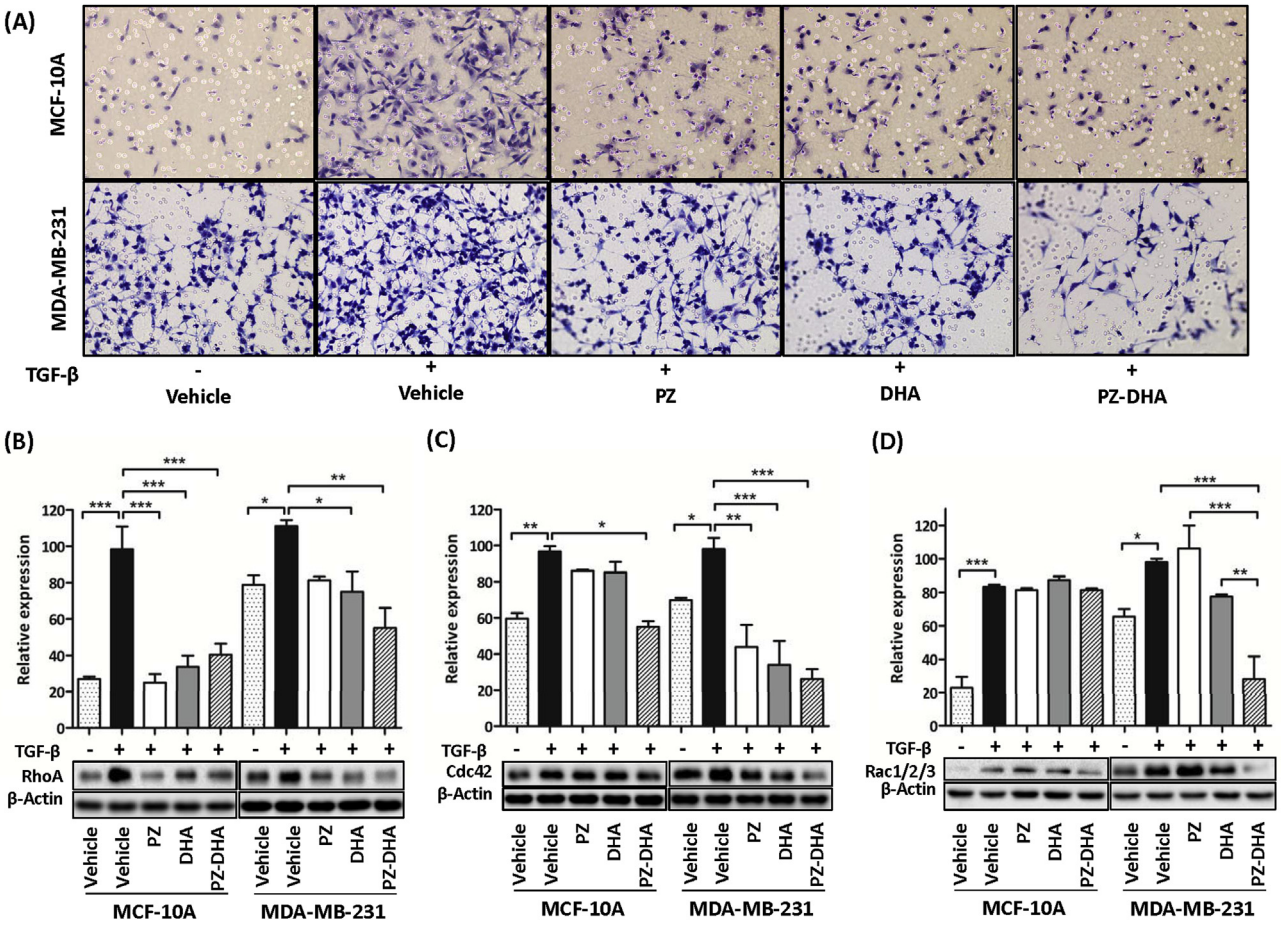

Fig. 3. PZ-DHA inhibits the expression of small GTPase proteins associated with TGF-β-induced cell migration. **(A)** MCF-10A or MDA-MB-231 cells were pre-treated with 10 ng/mL TGF-β and then exposed to PZ, DHA, PZ-DHA (20 μM) or vehicle alone for 24 h in the presence or absence of 5 ng/mL TGF-β. Treated cells were serum-starved and resuspended in serum-free F12/DMEM or DMEM and their chemoattractant-induced migration was determined. **(B, C, D)** MCF-10A and MDA-MB-231 cells that were treated with or without 10 ng/mL TGF-β were then exposed to PZ, DHA, PZ-DHA (20 μM) or vehicle alone in the presence or absence of 5 ng/mL TGF- β for 72 h. Relative expression ± SEM of 3 independent experiments of TGF-β-induced **(B)** RhoA, **(C)** Cdc42 and **(D)** Rac1/2/3 was determined using Western blot analysis. Equal protein loading was confirmed by β-actin expression. Differences between means were compared by ANOVA with Tukey's multiple comparisons test; *P < 0.05, **P < 0.01 and ***P < 0.001.

Moreover, expression of MMP-2, which degrades gelatin and fibronectin of the ECM [31], was diminished when MDA-MB-231 cells were cultured for 72 h in the presence of sub-cytotoxic PZ-DHA (Fig. 2H). DHA alone had a weaker but statistically significant inhibitory effect on MDA-MB-231 invasion through gelatin and MMP-2 expression, which was not seen with PZ alone. Taken together, these findings suggest a potent inhibitory effect of sub-cytotoxic PZ-DHA on the invasive capacity of TNBC cells, possibly via decreased expression of MMP-2.

Since RhoA, Cdc42, and Rac expression is associated with cell migration via the formation of lamellipodia and filopodia [32], we next tested the effect of PZ-DHA on the TGF-β-induced expression of these small GTPase proteins by MCF-10A mammary epithelial cells and MDA-MB-231 TNBC cells. As expected, TGF-β stimulated the migration of MCF-10A and MDA-MB-231 cells, which was inhibited by PZ, DHA, and PZ-DHA, with PZ-DHA having the greatest inhibitory effect (Fig. 3A). TGF-β also induced the expression of RhoA and Cdc42 by MCF-10A and MDA-MB-231 cells; however, there was a significant reduction in TGF-β-induced RhoA (Fig. 3B) and Cdc42 (Fig. 3C) expression relative to the vehicle control after 72 h culture in the presence of PZ-DHA. TGF-β-induced Rac1/2/3 expression was decreased in MDA-MB-231 cells but not MCF-10A cells following PZ-DHA treatment (Fig. 3D). In MDA-MB-231 cell cultures, PZ-DHA had a greater effect than either PZ or DHA alone whereas this was not always the case in MCF-10A cell cultures. Treatment with PZ-DHA or DHA alone also caused a reduction in basal expression of RhoA and Cdc42, but not Rac1/2/3 by MDA-MB-231 cells (see Supplementary Fig. 2).

3.3. PZ-DHA inhibits EMT of MDA-MB-231 and SUM149 cells

EMT, which involves the β-catenin-induced expression of transcription factors belonging to the ZEB, Snail/Slug, and Twist families, as well as their downstream targets E-cadherin and vimentin, is a contributing factor in carcinoma progression, including metastasis [33]. We therefore determined the impact of PZ-DHA treatment on the expression of EMT-associated proteins by MDA-MB-231 and SUM149 TNBC cells. As shown in Fig. 4, MDA-MB-231 cells that were cultured in the presence of PZ-DHA for 72 h exhibited a reduction in the expression of β-catenin (Fig. 4A), Slug (Fig. 4B) and ZEB-1 (Fig. 4C), as well as increased the expression of epithelial marker, E-cadherin (Fig. 4G); however, inhibition of vimentin (Fig. 4D) and N-cadherin (Fig. 4G) expression by PZ-DHA, although consistent from experiment to experiment, did not achieve statistical significance. PZ-DHA inhibited SUM149 cell expression of Slug (Fig. 4E) and vimentin (Fig. 4F), as well as causing increased expression of E-cadherin and decreased N-cadherin expression (Fig. 4H). Neither PZ nor DHA alone had any significant effect on the expression of these EMT-associated proteins by MDA-MB-231 cells; however, DHA alone showed some inhibition of Slug and

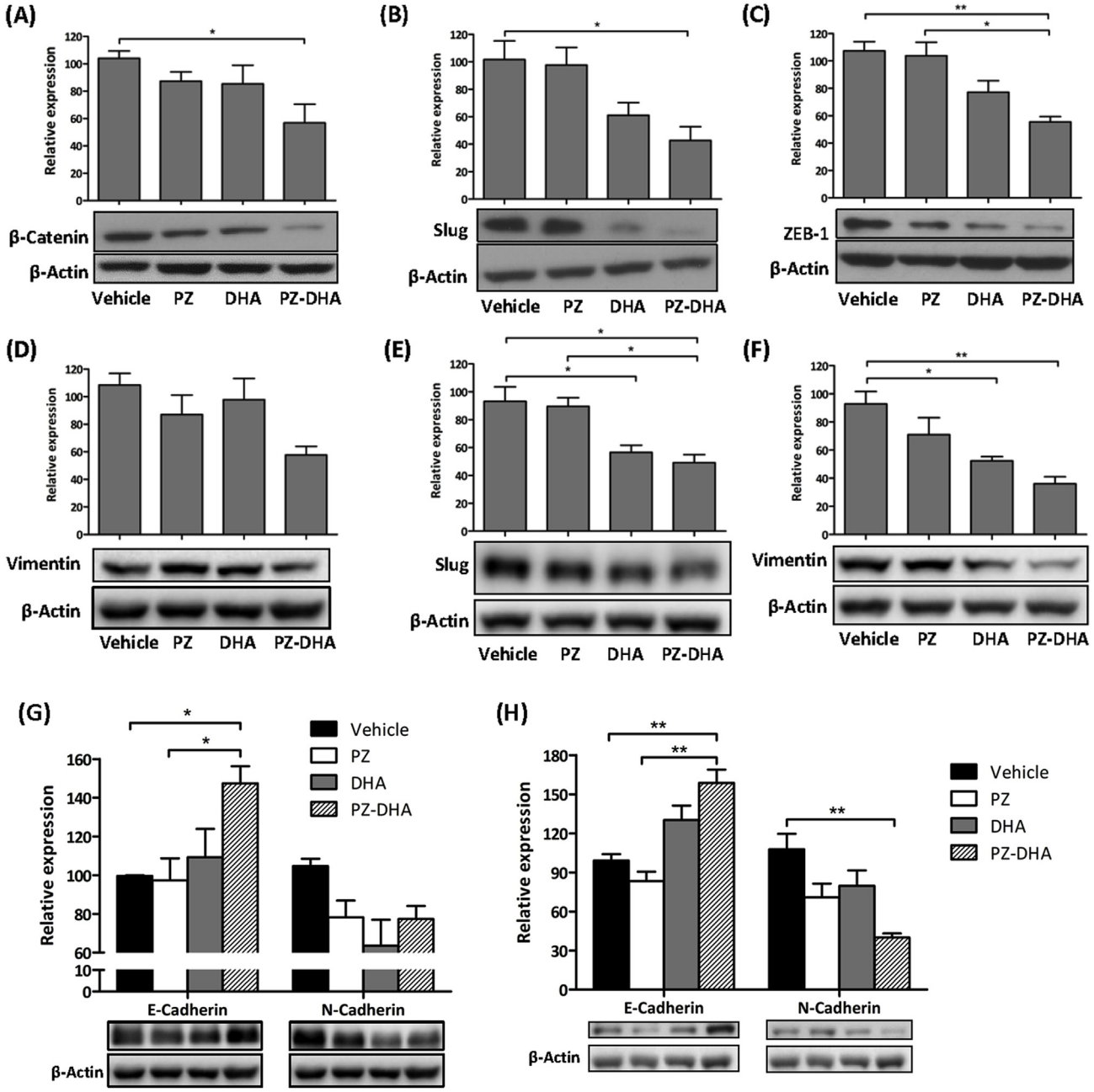

Fig. 4. PZ-DHA inhibits EMT-associated protein expression in TNBC cells. MDA-MB-231 or SUM149 cells were cultured for 72 h in the presence of PZ, DHA, PZ-DHA (20 μM) or vehicle alone. EMT-associated protein expression was then determined by western blotting. MDA-MB-231 expression of **(A)** β-catenin **(B)** Slug, **(C)** ZEB-1, **(D)** vimentin, and **(G)** E-cadherin/N-cadherin, and SUM149 expression of **(E)** Slug, **(F)** vimentin, and **(H)** E-cadherin/N-cadherin were determined. Equal protein loading was confirmed by β-actin expression. Data shown are mean relative expression ± SEM of 3–4 independent experiments. Differences between means were compared by ANOVA with Tukey's multiple comparisons test; *P < 0.05, and **P < 0.01.

vimentin expression by SUM149 cells.

3.4. PZ-DHA inhibits Akt/PI3K and MAPK signaling pathways of MDA-MB-231 cells

We next tested the effect of sub-cytotoxic PZ-DHA on Akt/PI3K and MAPK signaling pathways, both of which have been implicated in EMT and, by association, metastasis of TNBC cells [34,35]. Fig. 5 shows that 72 h culture of MDA-MB-231 TNBC cells in the presence of sub-cytotoxic PZ-DHA resulted in upregulation of PTEN phosphorylation (Fig. 5A), which is an upstream inhibitor of Akt/PI3K signaling [36], whereas the phosphorylation of PDK1 (Fig. 5B), which is an upstream inducer of Akt/PI3K signaling, was downregulated. Furthermore, reduced Akt/PI3K signaling was evident by decreased phosphorylation of the downstream effector molecule, mTOR (Fig. 2C). PZ and DHA alone inhibited PDK1 phosphorylation but not PTEN or mTOR phosphorylation. PZ-DHA also inhibited the phosphorylation of c-RAF and p44/p42 (ERK1/2) components of the MAPK signaling cascade (Fig. 5D and E, respectively), activation of which has been implicated in breast cancer progression [37]. DHA alone inhibited the phosphorylation of cRAF. Phosphorylation of p44/p42 was inhibited by both PZ and DHA alone, although not to the extent seen with PZ-DHA. We also examined the effect of PZ-DHA on the activation status of GSK3β, which can impact cancer progression and is regulated by several kinases including Akt and ERKs [38]. Consistent with our other findings, inhibitory phosphorylation of GSK3β at Ser9 was increased in the presence of PZ-

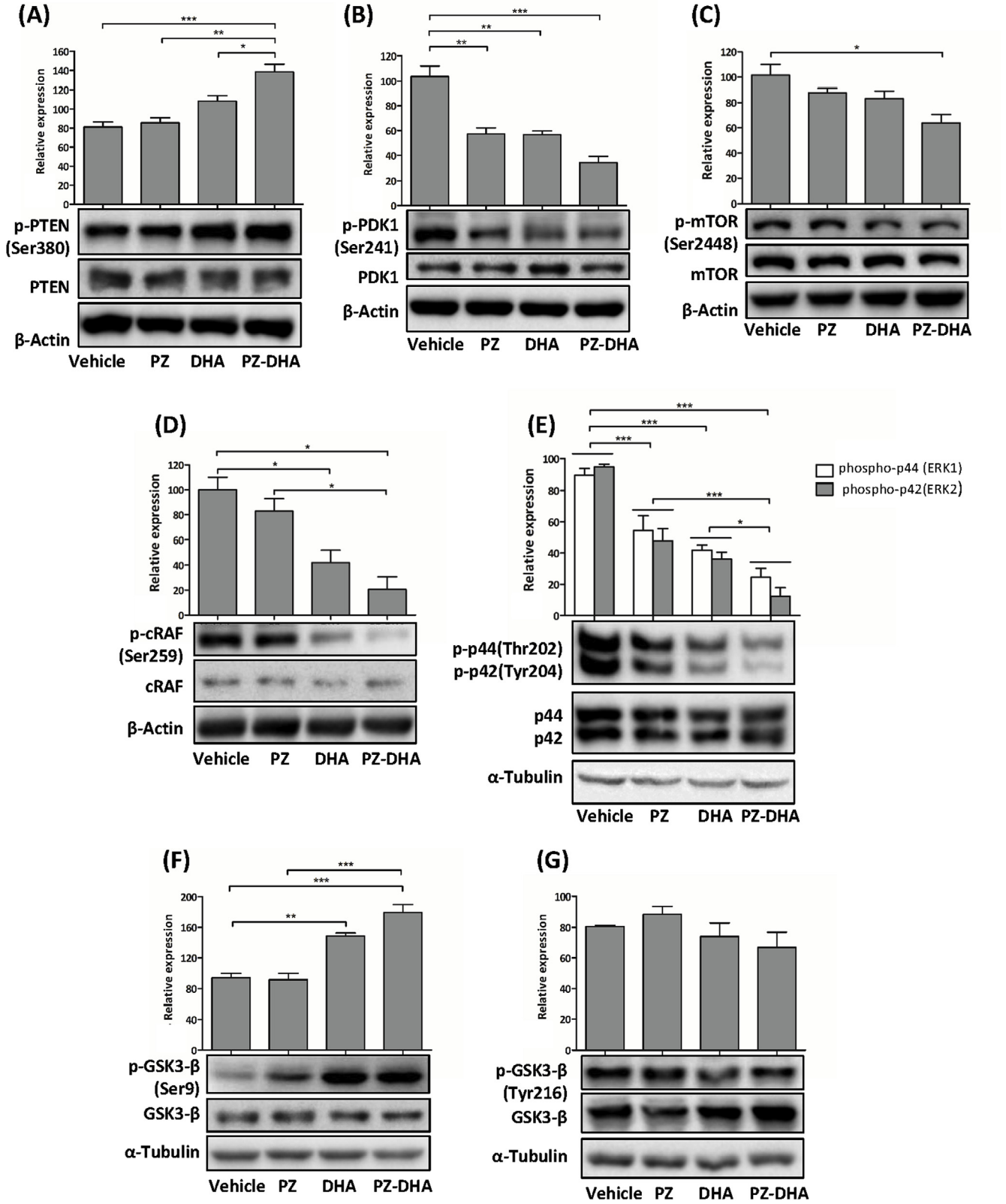

Fig. 5. PZ-DHA inhibits Akt/PI3K and MAPK signaling in TNBC cells. MDA-MB-231 cells were cultured for 72 h in the presence of PZ, DHA, PZ-DHA (20 μM) or vehicle alone. At the end of culture protein-rich cell lysates were prepared. Equal amounts of protein (20 μg) were loaded onto SDS-polyacrylamide gels and electrophoresed. Proteins were transferred to nitrocellulose membranes and blots probed for **(A)** phospho (p)-PTEN (Ser380)/total-PTEN, **(B)** p-PDK1 (Ser241)/total-PDK1, **(C)** p-mTOR (Ser2448)/total-mTOR, **(D)** p-cRAF (Ser259)/total-cRAF, **(E)** p-p44 (Thr202)/p42 (Tyr204)/total-p44/p42, **(F)** p-GSK3β (Ser9)/total-GSK3β, and **(G)** p-GSK3β (Tyr216)/total-GSK3β. Equal protein loading was confirmed by β-actin or α-tubulin expression. Data shown are mean relative expression ± SEM of 3 independent experiments. Statistical significance was determined by ANOVA and the Tukey post-test; *P < 0.05, **P < 0.01 and ***P < 0.001.

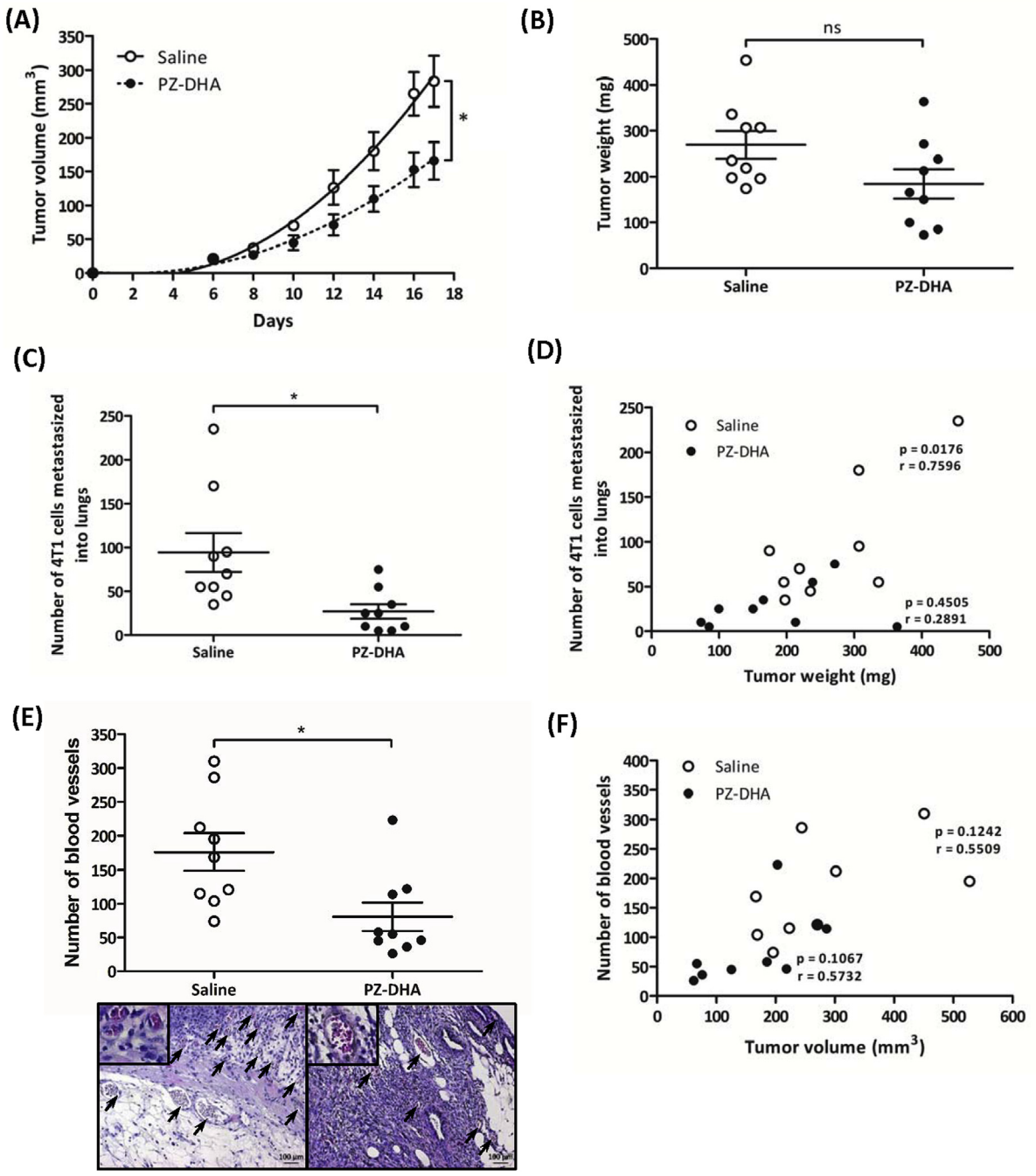

Fig. 6. PZ-DHA suppresses 4T1 tumor growth and metastasis in immune-competent mice. 4T1 mouse mammary carcinoma cells were injected into the left inguinal mammary fat pad of syngeneic female BALB/c mice and saline or PZ-DHA (100 mg/kg) were administered by intraperitoneal injection every second day beginning at day 8 after implantation. On day 17, mice were euthanized and primary tumors were removed. **(A)** Tumor volumes were determined by caliper measurements every second day and are shown as mean (mm^3) ± SEM. **(B)** Tumor weights (wet) at day 17 are shown as mean (mg) ± SEM. **(C)** Lungs were harvested, minced and the number of lung metastases at day 17 were determined by colony-forming assay. Data are shown as mean # metastases ± SEM. **(D)** Correlation of primary tumor weight to number of 4T1 cells metastasized into lungs was determined using the Pearson correlation statistical method. **(E)** Blood vessels (indicated by arrows) in the primary tumors were counted on a hematoxylin and eosin stained section (see representative sections). Data are shown as mean # blood vessels ± SEM. **(F)** Correlation of primary tumor volume to number of tumor associated-blood vessels was determined using the Pearson correlation statistical method. Statistical differences between means were compared by Student's t-test; *P < 0.05.

DHA, as well as DHA alone (Fig. 5F), whereas there was no change in phosphorylation at Tyr216 (Fig. 5G), indicating inhibition of GSK3β activity.

3.5. PZ-DHA suppresses 4T1 and MDA-MB-231 tumor growth and metastasis in mice

To determine whether the *in vitro* inhibition of metastatic activities and metastasis-associated signaling pathways extended to the tumor microenvironment, we implanted 4T1 mammary carcinoma cells into immune-competent BALB/c female mice and MDA-MB-231 breast

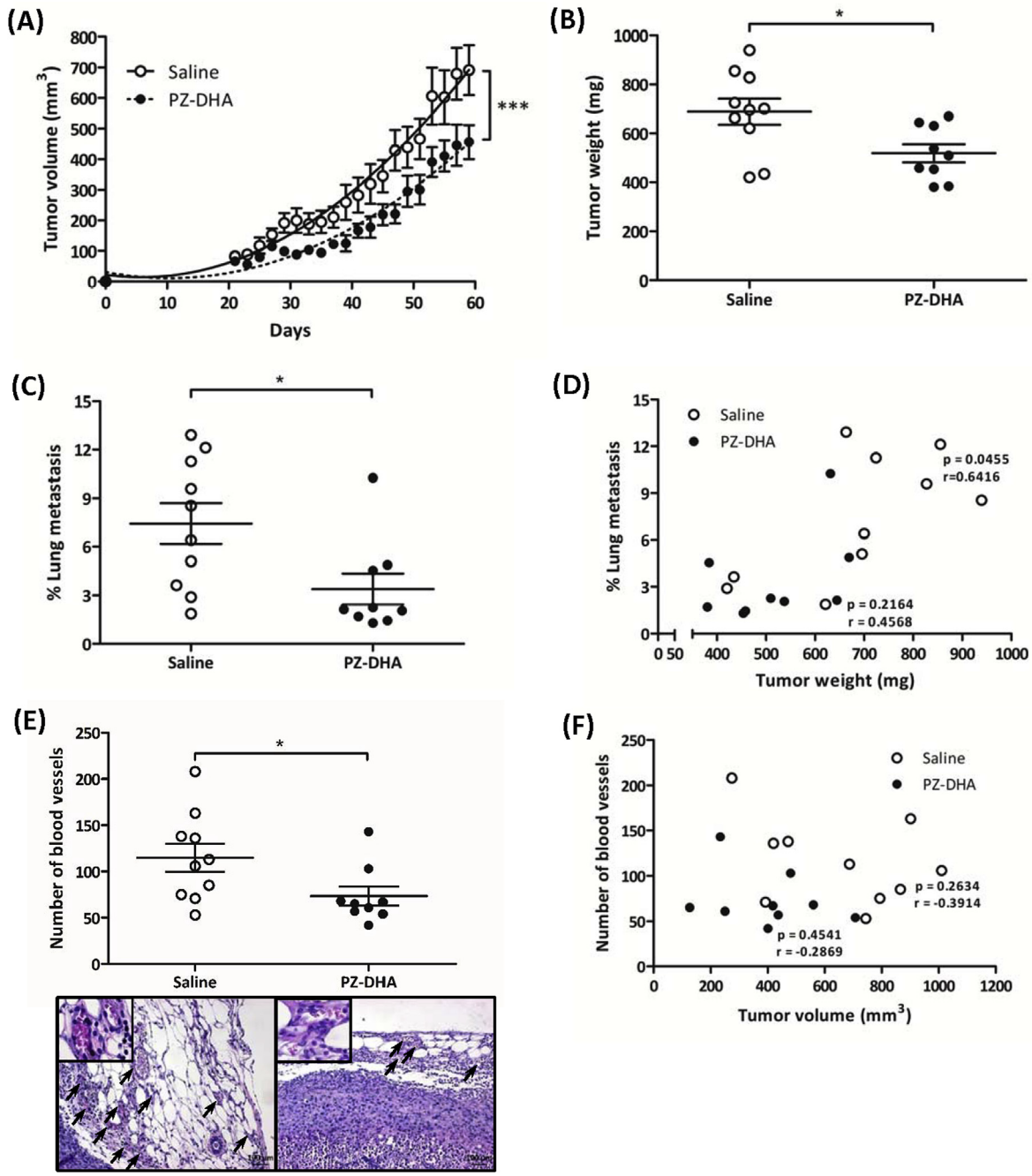

Fig. 7. PZ-DHA suppresses MDA-MB-231 tumor xenograft growth and metastasis in immune-deficient mice. GFP-tagged MDA-MB 231 breast cancer cells were mixed with Matrigel and injected into the left inguinal mammary fat pad of female NOD-SCID mice and saline or PZ-DHA (100 mg/kg) were administered by intraperitoneal injection every second day beginning at day 21. On day 59, mice were euthanized and primary tumors were removed. **(A)** Tumor volumes were determined by caliper measurements every second day and are shown as mean (mm^3) ± SEM. **(B)** Tumor weights (wet) at day 59 are shown as mean (mg) ± SEM. Tumor weights were recorded and data are shown as mean (mg) ± SEM. **(C)** Lungs were harvested, minced and the resulting single cell suspensions were analyzed by flow cytometry to determine % lung metastasis, denoted as mean ± SEM. **(D)** Correlation of primary tumor weight to MDA-MB-231 metastases in the lungs was determined using the Pearson correlation statistical method. **(E)** Blood vessels (indicated by arrows) in the primary tumors were counted on a hematoxylin and eosin stained section (see representative sections). Data are shown as mean # blood vessels ± SEM. **(F)** Correlation of primary tumor volume to number of tumor associated-blood vessels was determined using the Pearson correlation statistical method. Statistical differences between means were compared by Student's t-test; *P < 0.05.

cancer cells into immune-deficient NOD-SCID mice. Both groups of mice subsequently received saline or PZ-DHA by intraperitoneal injection. As shown in Figs. 6 and 7, PZ-DHA-treated mice experienced a reduction in primary tumor volume (4T1, Fig. 6A; MDA-MB-231, Fig. 7A). PZ-DHA treatment also reduced MDA-MB-231 tumor weight (Fig. 7B); however, 4T1 tumor weight was not affected (Fig. 6B). Importantly, mice that were treated with PZ-DHA experienced a significant reduction in metastasis of 4T1 (Fig. 6C) and MDA-MB-231 (Fig. 7C) mammary carcinoma cells into the lungs. Inhibition of lung metastases development did not correlate with the effect of PZ-DHA on primary tumor growth (4T1, Fig. 6D; MDA-MB-231, Fig. 7D), suggesting that suppression of primary tumor growth was not the cause of

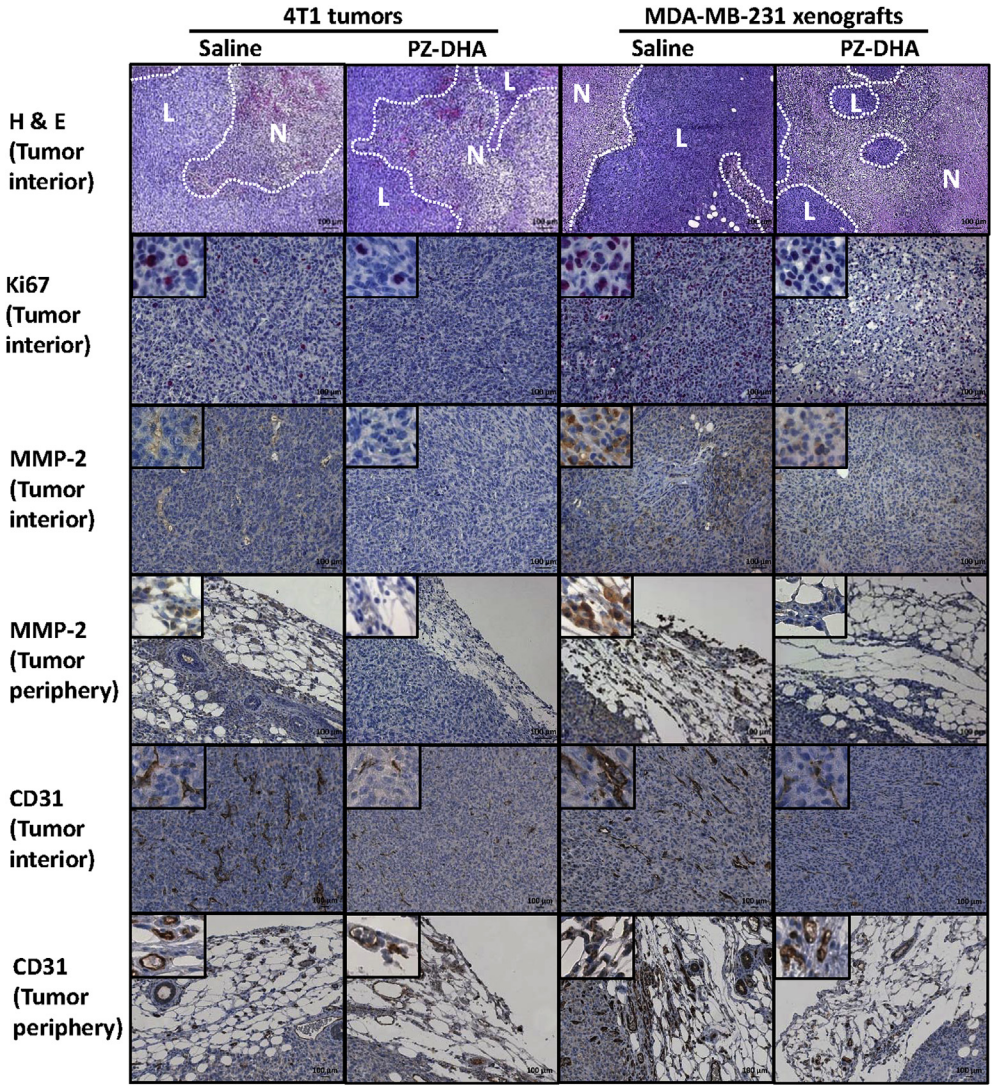

Fig. 8. PZ-DHA decreases Ki67, MMP-2 and CD31 expression in primary 4T1 and MDA-MB-231 tumors. Fixed tumor sections from saline- and PZ-DHA-treated mice were stained with hematoxylin and eosin to identify regions of necrosis and tumor-associated blood vessels, L: live tissue and N: necrotic tissue. Deparaffinized tumor sections were also stained with mouse monoclonal anti-Ki67, mouse monoclonal anti-MMP-2, or rabbit monoclonal anti-CD31 Abs. MMP-2 and CD31-staining was visualized with mouse-on-mouse HRP-polymer and the HRP/DAB detection system. Ki67-staining was visualized with MACH 4 MR AP polymer and a Vulcan fast red chromogen kit 2. Representative tumor sections photographed at × 200 and × 400 magnification are shown. (For interpretation of the references to colour in this figure legend, the reader is referred to the Web version of this article.)

Table 1
PZ-DHA does not cause liver or kidney toxicity[a].

Serum parameter	Saline	PZ-DHA
ALT (U/ml)	0.013 ± 0.002	0.012 ± 0.002*
Creatinine (μM)	61.7 ± 3.3	62.3 ± 3.8*

[a] Serum levels of ALT and creatinine were determined following treatment of female BALB/c mice with saline or 100 mg/kg PZ-DHA, every second day for 9 days (5 doses). Data are shown as the average value ± SEM. Statistical significance was determined by Student's t-test; *P > 0.05, i.e. not significant.

reduced metastasis to the lungs. In addition, treatment with PZ-DHA caused a significant decrease in the number of blood vessels in the primary tumor (4T1, Fig. 6E; MDA-MB-231, Fig. 7E), which was also independent of primary tumor growth. As shown in Fig. 8, immunohistochemical analysis of fixed 4T1 and MDA-MB-231 tumor sections from PZ-DHA-treated mice showed a decrease in Ki67, MMP-2 and CD31 expression, which was consistent with PZ-DHA-induced suppression of tumor growth (Ki67), metastatic activity (MMP-2), and development of tumor-associated blood vessels (CD31). There was no evidence of toxicity due to PZ-DHA treatment since both liver and kidney function remained normal, as assessed by serum ALT and creatinine levels (Table 1). Moreover, the behavior of the tumor-bearing mice was not altered by PZ-DHA treatment and necropsies did not reveal any gross anatomical differences between saline- and PZ-DHA-treated animals.

4. Discussion

Although recent advances in anticancer drug development have improved the initial treatment of cancer, metastasis remains the cause of nearly 90% of cancer-related deaths [39]. One approach to the development of new and more effective treatments for metastatic disease has been the investigation of plant-derived polyphenols for anti-metastatic properties; however, reports on pre-clinical or clinical applications are limited due to the in general poor bioavailability of these natural compounds. We have previously shown that PZ-DHA, a novel fatty acid ester derivative of a plant polyphenol, is selectively cytotoxic for TNBC cells [30]. In the present investigation, we establish, for the first time, that sub-cytotoxic PZ-DHA (≤ 20 μM) inhibited the *in vitro* and *in vivo* metastatic activity of TNBCs.

Invasion of adjacent tissues by tumor cells and their subsequent hematogenic and/or lymphogenic spread to distant sites involves tumor cell locomotion and the degradation of ECM components by proteolytic enzymes secreted by cancer cells and other cells in the tumor microenvironment [40]. PZ-DHA, at a concentration that was not cytotoxic for of triple-negative MDA-MB-231, SUM149, and 4T1 mammary carcinoma cells, inhibited the migration of these highly metastatic tumor cells in gap closure and transwell migration assays. Chemoattractant-directed migration of MDA-MB-231 TNBC cells across transwell

membranes coated with extracellular matrix proteins (gelatin or fibronectin) was also inhibited by sub-cytotoxic PZ-DHA, suggesting a suppressive effect on the invasion component of the metastatic process. Diminished tumor cell locomotion in the presence of PZ-DHA can be attributed to a concomitant reduction in RhoA and Cdc42 expression, which are GTPases that signal for actin polymerization during cell migration [32]. Moreover, Rho GTPase signaling is dysregulated in many cancers [41]. PZ-DHA also inhibited TGF-β-induced expression of RhoA and Cdc42 by MCF-10A normal mammary epithelial cells, as well as MDA-MB-231 TNBC cells, suggesting an effect at the level of TGF-β signaling, which is a key regulator of tumor progression [42,43]. Interestingly, exposure to PZ-DHA caused a reduction in TGF-β-induced Rac1/2/3 expression by MDA-MB-231 cells, but not MCF-10A cells, indicating a possible selective effect on neoplastic cells. It is noteworthy that MMP-2 expression by MDA-MB-231 cells was diminished following treatment with sub-cytotoxic PZ-DHA. This finding was consistent with reduced chemoattractant-directed migration of PZ-DHA-treated MDA-MB-231 cells across gelatin- or fibronectin-coated membranes since MMP-2 degrades both gelatin and fibronectin components of the ECM [31]. Moreover, MMP-2 is frequently overexpressed in breast tumor tissue and has been implicated in breast cancer metastasis [44]; therefore, MMP-2 inhibition by PZ-DHA has potential clinical implications.

The acquisition of migratory and invasive properties by carcinoma cells during tumor progression has been linked to EMT and the activation of EMT-associated signaling pathways [45]. Central to EMT is the β-catenin-induced expression of ZEB, Snail/Slug, and Twist family transcription factors, as well as their downstream targets E-cadherin and vimentin [33]. Activation of EMT-associated transcription factors in malignant epithelial cells, including mammary carcinoma cells, causes the loss of epithelial markers and stabilization of the mesenchymal phenotype [46]. Exposure of MDA-MB-231 TNBC cells to sub-cytotoxic PZ-DHA resulted in reduced expression of Slug and ZEB-1 transcription factors, as well as the reversal of EMT-induced depletion of E-cadherin. Sub-cytotoxic PZ-DHA had similar effects on Slug and E-cadherin expression by SUM149 cells. Reduced expression of vimentin and N-cadherin was also seen in PZ-DHA-treated SUM149 cells, and a consistent, although not statistically significant, reduction in MDA-MB-231 expression of vimentin and N-cadherin was noted in the presence of PZ-DHA. These findings are in line with decreased expression of β-catenin and EMT-associated transcription factors. PZ-DHA-mediated inhibition of Slug and ZEB-1 expression can be attributed to the concomitant β-catenin inhibition since β-catenin is a known inducer of these EMT-associated transcription factors [33].

Sub-cytotoxic PZ-DHA inhibited Akt/PI3K and MAPK signaling pathways that are involved in EMT and promote metastasis [34,35]. Treatment of MDA-MB-231 TNBC cells with PZ-DHA impacted upstream regulators of Akt/PI3K signaling [36], as evidenced by increased phosphorylation of inhibitory PTEN at Ser380 and decreased phosphorylation of stimulatory PDK1 at Ser241. Moreover, mTOR phosphorylation, which occurs downstream of Akt/PI3K signaling, was reduced in PZ-DHA-treated cells. Activation of c-RAF and ERK1/2 components of the MAPK signaling cascade was also inhibited in the presence of PZ-DHA, which is an important finding in light of the role of MAPK in breast cancer progression [37]. Moreover, an overall reduction in GSK3β kinase activity, which is regulated by several kinases including Akt and ERKs [38], was evident in PZ-DHA-treated MDA-MB-231 cells since there was increased phosphorylation of GSK3β at Ser9 (inhibits GSK3β) but no change in GSK3β phosphorylation at Tyr216 (activates GSK3β). There are at least two distinct pools of GSK3β present in a cell, one being resistant to phosphorylation by Akt and the other being regulated by Akt-induced kinase activity [47]. However, at this time it is not clear whether PZ-DHA-induced phosphorylation of GSK3β at Ser9 in MDA-MB-231 cells was responsible for reduced expression of β-catenin, which would, in turn, inhibit the expression of EMT-associated genes, as described in MCF-7 breast cancer cells [48]. Nevertheless, taken together, our data suggest that the Akt/PI3K and ERK1/2 signal transduction pathways are important targets for PZ-DHA. In agreement with earlier studies [49,50], DHA by itself inhibited Akt/PI3K and MAPK signaling, as did PZ, albeit to a lesser extent than PZ-DHA.

Although we have evidence that PZ-DHA is taken up by both malignant and normal cells, at this time the precise intracellular target of PZ-DHA is not known. Indeed, the intracellular targets in cancer cells for most, if not all, bioactive phytochemicals that suppress the growth of cancer cells have not yet been identified. It has been suggested that dietary ω-3-fatty acids such as DHA inhibit breast cancer cell proliferation by acting at the level of G protein-coupled receptors (GPR40 and GPR120) in the free fatty acid receptor family [51]. However, GPR120 activation in breast cancer cells has recently been reported to promote metastasis via Akt/PI3K signaling [52], which argues against a role for GPR120 in mediating the anti-metastatic activity of PZ-DHA. Interestingly, PZ is a glycoside of phloretin, which functions as an estrogen receptor α antagonist [53]. However, any action of PZ-DHA via estrogen receptor α is ruled out by the fact that this receptor is not expressed by the TNBC cells used in our study [54]. The nature of the intracellular target for PZ-DHA therefore remains an important question for future study.

Consistent with our *in vitro* findings, systemic administration of PZ-DHA via intraperitoneal injections suppressed the growth of two aggressive types of mammary carcinoma cells and their metastasis to the lungs, without any evidence of adverse effects or acute toxicity in PZ-DHA-treated mice. Preliminary pharmacokinetic experiments suggest that PZ-DHA administered by intraperitoneal injections is absorbed directly into the circulation, after which PZ-DHA undergoes phase 1 and phase 2 metabolism. Immunohistochemical staining of sections from primary tumors revealed that expression of the proliferation marker Ki67 and metastasis-promoting MMP-2 was decreased as a result of PZ-DHA treatment, providing further evidence of *in vivo* anticancer activity by PZ-DHA. In addition, the reduced number of blood vessels and decreased expression of the endothelial cell marker CD31 expression in primary tumor sections from PZ-DHA-treated mice suggested an anti-angiogenic effect, which could impact both tumor growth and metastasis. However, neither the inhibition of metastasis nor the suppression of tumor-associated blood vessel development correlated with the growth of the primary tumor, suggesting that these effects were not the result of primary tumor growth inhibition by PZ-DHA. Taken together, our *in vivo* findings suggest that reduced ECM degradation and/or hematogenic dissemination of mammary carcinoma cells in PZ-DHA-treated mice contributed to the observed reduction in lung metastasis.

In conclusion, as depicted in Fig. 9, the current study reveals that sub-cytotoxic PZ-DHA inhibited multiple metastatic activities (migration, invasion, EMT) and metastasis-associated signaling pathways (TGFβ, Akt/PI3K, MAPK) in TNBC cells. Furthermore, a reduction in TGFβ, Akt/PI3K, and/or MAPK signaling following PZ-DHA treatment of TNBC cells may represent the molecular basis of the anti-metastatic effect of PZ-DHA. In light of the resistance of advanced metastatic TNBC to current chemotherapeutic regimens [1], our *in vitro* and *in vivo* findings suggest that PZ-DHA warrants further investigation as a potential drug candidate for the prevention and treatment of TNBC progression and metastasis.

Conflicts of interest

No conflicts to declare.

Funding

This research was funded by the Canadian Cancer Society/Canadian Breast Cancer Foundation-Atlantic Endowed Chair in Breast Cancer Research to DWH and a Natural Sciences and Engineering Research

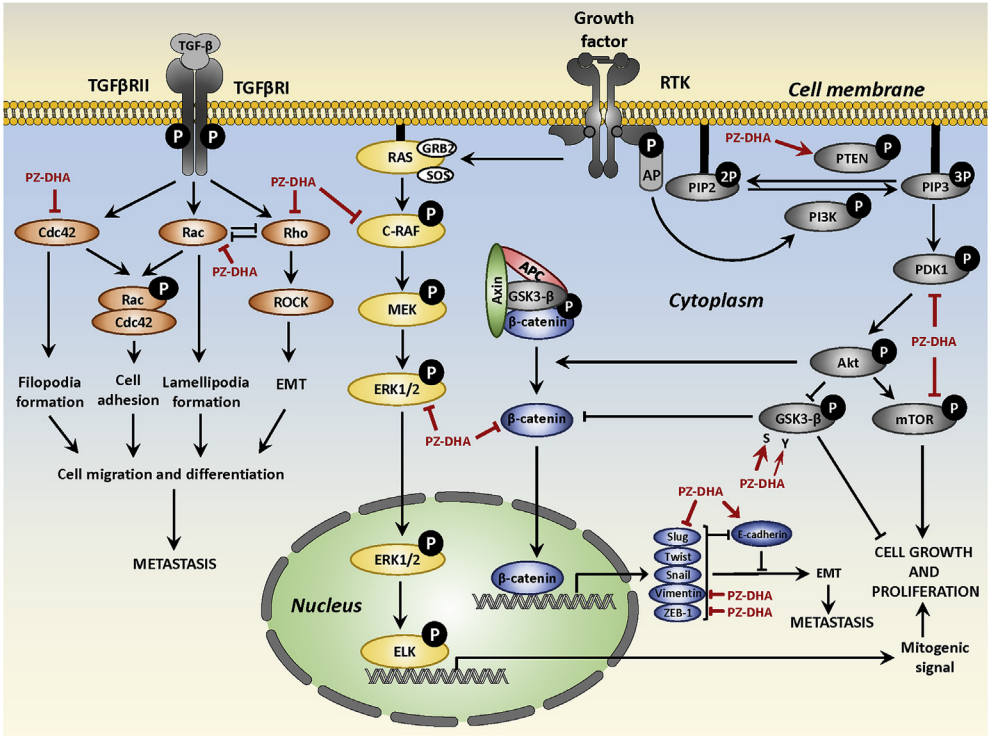

Fig. 9. Proposed model for anti-metastatic activities of sub-cytotoxic PZ-DHA. PZ-DHA inhibits TNBC cell migration and invasion, as well as metastasis and the expression of EMT-associated transcription factors. The molecular basis for these anti-metastatic effects of PZ-DHA involve the suppression of Akt/PI3K signaling by inducing the activation of Akt suppressor, PTEN, and inhibiting the phosphorylation-mediated activation of PDK1 and mTOR, as well as the down-stream effector GSK3-β. In addition, PZ-DHA suppresses MAPK activation by inhibiting the phosphorylation of RAS, c-RAF and ERK1/2. PZ-DHA-mediated inhibition of the EMT-associated transcription factor β-catenin results in the reduced expression of β-catenin-dependent EMT transcription factors such as Slug and ZEB-1, leading to increased expression of E-cadherin and inhibition of the metastatic cascade. PZ-DHA also inhibits TGF-β-induced expression of Cdc42, Rac1/2/3 and RhoA, which are also involved in cell migration and EMT.

Akt: Protein kinase B; **AP:** Activator protein; **APC:** Adenomatous polyposis coli; **c-RAF:** Proto-oncogene serine/threonine-protein kinase; **ELK:** ETS domain-containing protein; **EMT:** Epithelial-to-mesenchymal transition; **ERK1/2:** Extracellular signal–regulated kinases1/2; **GSK3-β**: Glycogen synthase kinase 3-β; **MEK:** Serine/tyrosine/threonine kinase; **mTOR:** mammalian target of rapamycin; **PDK1**: Phosphoinositide-dependent kinase-1; **PI3K:** Phosphoinositide 3-kinase; **PIP2:** Phosphatidylinositol (4,5)-bisphosphate; **PIP3:** Phosphatidylinositol (3,4,5)-trisphosphate; **PTEN:** Phosphatase and tensin homolog; **PZ-DHA:** Phloridzin docosahexaenoate; **RAS, Cdc42, Rac1/2/3** and **RhoA:** Small GTPases; **ROCK**: Rho-associated protein kinase; **RTK:** Receptor tyrosine kinase; **TGF-β**: Transforming growth factor-β; **TGFβR**: Transforming growth factor-β receptor; **ZEB1:** Zinc finger E-box-binding homeobox.

Council Discovery Grant to HPVR. WF is a trainee in the Cancer Research Training Program of the Beatrice Hunter Cancer Research Institute, with funds provided by the CIBC Graduate Scholarship in Medical Research and the Dalhousie Medical Research Foundation Edward F. Crease Memorial Graduate Studentship in Cancer Research.

Acknowledgements

We would like to thank Dr. Melanie R. Power Coombs and Dr. Anna L. Greenshields for their intellectual contributions and Pat Colp for assistance with immunohistochemistry.

Appendix A. Supplementary data

Supplementary data to this article can be found online at https://doi.org/10.1016/j.canlet.2019.08.015.

References

[1] W.D. Foulkes, I.E. Smith, J.S. Reis-Filho, Triple-negative breast cancer, N. Engl. J. Med. 363 (2010) 1938–1948, https://doi.org/10.1056/NEJMra1001389.
[2] X. Jin, P. Mu, Targeting breast cancer metastasis, Breast Canc. 9 (2015) 23–34, https://doi.org/10.4137/BCBCR.S25460.
[3] B. Yücel, S. Bahar, T. Kaçan, M.M. Şeker, M.G. Celasun, A. Bahçeci, N.A. Babacan, Importance of metastasis site in survival of patients with breast cancer, Austin J. Med. Oncol. 1 (2014) 1–7.
[4] M.C. Cummings, P.T. Simpson, L.E. Reid, J. Jayanthan, J. Skerman, S. Song, A.E. McCart Reed, J.R. Kutasovic, A.L. Morey, L. Marquart, P. O'Rourke, S.R. Lakhani, Metastatic progression of breast cancer: insights from 50 years of autopsies, J. Pathol. 232 (2014) 23–31, https://doi.org/10.1002/path.4288.
[5] P. Burbelo, A. Wellstein, R.G. Pestell, Altered Rho GTPase signaling pathways in breast cancer cells, Breast Canc. Res. Treat. 84 (2004) 43–48, https://doi.org/10.1023/B:BREA.0000018422.02237.f9.
[6] C. Zhu, X. Qi, Y. Chen, B. Sun, Y. Dai, Y. Gu, PI3K/Akt and MAPK/ERK1/2 signaling pathways are involved in IGF-1-induced VEGF-C upregulation in breast cancer, J. Cancer Res. Clin. Oncol. 137 (2011) 1587–1594, https://doi.org/10.1007/s00432-011-1049-2.
[7] H. Ebi, C. Costa, A.C. Faber, M. Nishtala, H. Kotani, D. Juric, P. Della Pelle, Y. Song, S. Yano, M. Mino-Kenudson, C.H. Benes, J.A. Engelman, PI3K regulates MEK/ERK signaling in breast cancer via the Rac-GEF, P-Rex1, Proc. Natl. Acad. Sci. U.S.A. 110 (2013) 21124–21129, https://doi.org/10.1073/pnas.1314124110.
[8] M. Fedele, L. Cerchia, G. Chiappetta, The epithelial-to-mesenchymal transition in breast cancer: focus on basal-like carcinomas, Cancers 9 (2017) 134, https://doi.org/10.3390/cancers9100134.
[9] F. van Zijl, G. Krupitza, W. Mikulits, Initial steps of metastasis: cell invasion and endothelial transmigration, Mutat. Res. 728 (2011) 23–34, https://doi.org/10.1016/j.mrrev.2011.05.002.
[10] M. Parri, P. Chiarugi, Rac and Rho GTPases in cancer cell motility control, Cell Commun. Signal. 8 (2010) 23, https://doi.org/10.1186/1478-811X-8-23.
[11] A.G. Clark, D.M. Vignjevic, Modes of cancer cell invasion and the role of the microenvironment, Curr. Opin. Cell Biol. 36 (2015) 13–22, https://doi.org/10.1016/J.CEB.2015.06.004.
[12] A. Moustakas, P. Heldin, TGFβ and matrix-regulated epithelial to mesenchymal transition, Biochim. Biophys. Acta Gen. Subj. 1840 (2014) 2621–2634, https://doi.org/10.1016/J.BBAGEN.2014.02.004.
[13] T. Doo, G. Maskarinec, Polyphenols and breast cancer prevention: a summary of the epidemiologic evidence, in: R.R. Watson, V.R. Preedy, S. Zibadi (Eds.), Polyphenols in Human Health and Disease, Elsevier, 2013, pp. 1331–1340, , https://doi.org/10.1016/B978-0-12-398456-2.00100-6.
[14] A. Abdal Dayem, H.Y. Choi, G.-M. Yang, K. Kim, S.K. Saha, S.-G. Cho, The anti-cancer effect of polyphenols against breast cancer and cancer stem cells: molecular mechanisms, Nutrients 8 (2016) 581, https://doi.org/10.3390/nu8090581.
[15] T. Sun, Q.Y. Chen, L.J. Wu, X.M. Yao, X.J. Sun, Antitumor and antimetastatic activities of grape skin polyphenols in a murine model of breast cancer, Food Chem. Toxicol. 50 (2012) 3462–3467, https://doi.org/10.1016/J.FCT.2012.07.037.
[16] P. Obakan-Yerlikaya, E.D. Arisan, A. Coker-Gurkan, N. Palavan-Unsal, Breast cancer and flavonoids as treatment strategy, in: P.V. Pham (Ed.), Breast Cancer - from Biology to Medicine, IntechOpen, 2017, , https://doi.org/10.5772/66169.
[17] A. Kozłowska, D. Szostak-Wegierek, Flavonoids–food sources and health benefits, Rocz. Panstw. Zakl. Hig. 65 (2014) 79–85.
[18] C. Hui, X. Qi, Z. Qianyong, P. Xiaoli, Z. Jundong, M. Mantian, Flavonoids, flavonoid subclasses and breast cancer risk: a meta-analysis of epidemiologic studies, PLoS One 8 (2013), https://doi.org/10.1371/journal.pone.0054318 e54318.
[19] Z.-P. Xiao, Z.-Y. Peng, M.-J. Peng, W.-B. Yan, Y.-Z. Ouyang, H.-L. Zhu, Flavonoids health benefits and their molecular mechanism, Mini Rev. Med. Chem. 11 (2011) 169–177.
[20] W.-J. Yan, X.-C. Ma, X.-Y. Gao, X.-H. Xue, S.-Q. Zhang, Latest research progress in the correlation between baicalein and breast cancer invasion and metastasis, Mol.

Clin. Oncol. 4 (2016) 472–476, https://doi.org/10.3892/mco.2016.750.
[21] F. Ni, Y. Gong, L. Li, H.M. Abdolmaleky, J.-R. Zhou, Flavonoid ampelopsin inhibits the growth and metastasis of prostate cancer in vitro and in mice, PLoS One 7 (2012), https://doi.org/10.1371/journal.pone.0038802 e38802.
[22] C.-J. Weng, G.-C. Yen, C.-J. Weng, G.-C. Yen, Flavonoids, a ubiquitous dietary phenolic subclass, exert extensive in vitro anti-invasive and in vivo anti-metastatic activities, Cancer Metastasis Rev. 31 (2012) 323–351, https://doi.org/10.1007/s10555-012-9347-y.
[23] C. Martínez-Pérez, C. Ward, A.K. Turnbull, P. Mullen, G. Cook, J. Meehan, E.J. Jarman, P.I.T. Thomson, C.J. Campbell, D. McPhail, D.J. Harrison, S.P. Langdon, Antitumour activity of the novel flavonoid Oncamex in preclinical breast cancer models, Br. J. Canc. 114 (2016) 905–916, https://doi.org/10.1038/bjc.2016.6.
[24] F. Li, C. Li, H. Zhang, Z. Lu, Z. Li, Q. You, N. Lu, Q. Guo, VI-14, a novel flavonoid derivative, inhibits migration and invasion of human breast cancer cells, Toxicol. Appl. Pharmacol. 261 (2012) 217–226, https://doi.org/10.1016/j.taap.2012.04.011.
[25] N. Yao, C.-Y. Chen, C.-Y. Wu, K. Motonishi, H.-J. Kung, K.S. Lam, Novel flavonoids with antiproliferative activities against breast cancer cells, J. Med. Chem. 54 (2011) 4339–4349, https://doi.org/10.1021/jm101440r.
[26] K.S. Bhullar Ziaullah, S.N. Warnakulasuriya, H.P.V. Rupasinghe, Biocatalytic synthesis, structural elucidation, antioxidant capacity and tyrosinase inhibition activity of long chain fatty acid acylated derivatives of phloridzin and isoquercitrin, Bioorg. Med. Chem. 21 (2013) 684–692, https://doi.org/10.1016/j.bmc.2012.11.034.
[27] S.V.G. Nair, Ziaullah, H.P.V. Rupasinghe, Fatty acid esters of phloridzin induce apoptosis of human liver cancer cells through altered gene expression, PLoS One 9 (2014), https://doi.org/10.1371/journal.pone.0107149 e107149.
[28] N. Arumuggam, N. Melong, C.K. Too, J.N. Berman, H.P.V. Rupasinghe, Phloridzin docosahexaenoate, a novel flavonoid derivative, suppresses growth and induces apoptosis in T-cell acute lymphoblastic leukemia cells, Am. J. Cancer Res. 7 (2017) 2452–2464.
[29] S. Sekhon-Loodu, Ziaullah, H.P.V. Rupasinghe, Docosahexaenoic acid ester of phloridzin inhibit lipopolysaccharide-induced inflammation in THP-1 differentiated macrophages, Int. Immunopharmacol. 25 (2015) 199–206, https://doi.org/10.1016/j.intimp.2015.01.019.
[30] W. Fernando, M.R.P. Coombs, D.W. Hoskin, H.P.V. Rupasinghe, Docosahexaenoic acid-acylated phloridzin, a novel polyphenol fatty acid ester derivative, is cytotoxic to breast cancer cells, Carcinogenesis 37 (2016) 1004–1013, https://doi.org/10.1093/carcin/bgw087.
[31] Y. Itoh, H. Nagase, Matrix metalloproteinases in cancer, Essays Biochem. 38 (2002) 21–36.
[32] S. Hanna, M. El-Sibai, Signaling networks of Rho GTPases in cell motility, Cell. Signal. 25 (2013) 1955–1961, https://doi.org/10.1016/j.cellsig.2013.04.009.
[33] S. Goossens, N. Vandamme, P. Van Vliergerghe, G. Berx, EMT transcription factors in cancer development re-evaluated: beyond EMT and MET, Biochim. Biophys. Acta Rev. Canc. 1868 (2017) 584–591, https://doi.org/10.1016/j.bbcan.2017.06.006.
[34] J. Li, X. Gong, R. Jiang, D. Lin, T. Zhou, A. Zhang, H. Li, X. Zhang, J. Wan, G. Kuang, H. Li, Fisetin inhibited growth and metastasis of triple-negative breast cancer by reversing epithelial-to-mesenchymal transition via PTEN/Akt/GSK3β signal pathway, Front. Pharmacol. 9 (2018) 722, https://doi.org/10.3389/fphar.2018.00772.
[35] C. Bartholomeusz, X. Xie, M.K. Pitner, K. Kondo, A. Dadbin, J. Lee, H. Saso, P.D. Smith, K.N. Dalby, N.T. Ueno, MEK inhibitor Selumetinib (AZ6244; ARRY-142886) prevents lung metastasis in a triple-negative breast cancer xenograft model, Mol. Cancer Ther. 14 (2015) 2773–2781, https://doi.org/10.1158/1535-7163.MCT-15-0243.
[36] S. Noorolyai, N. Shajari, E. Baghbani, S. Sadreddini, B. Baradaran, The relation between PI3K/AKT signalling pathway and cancer, Gene 689 (2019) 120–128, https://doi.org/10.1016/j.gene.2019.02.076.
[37] A. Adeyinka, Y. Nui, T. Cherlet, L. Snell, P.H. Watson, L.C. Murphy, Activated mitogen-activated protein kinase expression during human breast tumorigenesis and breast cancer progression, Clin. Cancer Res. 8 (2002) 1747–1753.
[38] J. Luo, The role of glycogen synthase kinase 3β (GSK3β) in tumorigenesis and cancer chemotherapy, Cancer Lett. 273 (2009) 194–200, https://doi.org/10.1016/j.can.let.2008.05.045.
[39] X. Guan, Cancer metastases: challenges and opportunities, Acta Pharm. Sin. B 5 (2015) 402–418, https://doi.org/10.1016/J.APSB.2015.07.005.
[40] L.A. Liotta, Gene products which play a role in cancer invasion and metastasis, Breast Canc. Res. Treat. 11 (1988) 113–124.
[41] A.P. Porter, A. Papaioannou, A. Malliri, Deregulation of Rho GTPases in cancer, Small GTPases 7 (2016) 123–138, https://doi.org/10.1080/21541248.2016.1173767.
[42] M.-F. Pang, A.-M. Georgoudaki, L. Lambut, J. Johansson, V. Tabor, K. Hagikura, Y. Jin, M. Jansson, J.S. Alexander, C.M. Nelson, L. Jakobsson, C. Betsholtz, M. Sund, M.C.I. Karlsson, J. Fuxe, TGF-β1-induced EMT promotes targeted migration of breast cancer cells through the lymphatic system by the activation of CCR7/CCL21-mediated chemotaxis, Oncogene 35 (2016) 748–760, https://doi.org/10.1038/onc.2015.133.
[43] P. Papageorgis, TGFβ signaling in tumor initiation, epithelial-to-mesenchymal transition, and metastasis, J. Oncol. 2015 (2015) 587193, https://doi.org/10.1155/2015/587193.
[44] A. Kohrmann, U. Kammerer, M. Kapp, J. Dietl, J. Anacker, Expression of matrix metalloproteinases (MMPs) in primary human breast cancer and breast cancer cell lines: new findings and review of the literature, BMC Canc. 9 (2009) 188, https://doi.org/10.1186/1471-2407-9-188.
[45] N.A. Gloushankova, I.Y. Zhitnyak, S.N. Rubtsova, Role of epithelial-mesenchymal transition in tumor progression, Biochemistry (Mosc.) 83 (2018) 1469–1476, https://doi.org/10.1134/S0006297918120052.
[46] Y. Wu, M. Sarkissyan, J. V Vadgama, Epithelial-mesenchymal transition and breast cancer, J. Clin. Med. 5 (2016) 13, https://doi.org/10.3390/jcm5020013.
[47] V.W. Ding, R.-H. Chen, F. McCormick, Differential regulation of glycogen synthase kinase 3β by insulin and Wnt signaling, J. Biol. Chem. 275 (2000) 32475–32481, https://doi.org/10.1074/jbc.M005342200.
[48] J.I. Yook, X.Y. Li, I. Ota, C. Hu, H.S. Kim, N.H. Kim, S.Y. Cha, J.K. Ryu, Y.J. Choi, J. Kim, E.R. Fearon, S.J. Weiss, A Wnt-Axin2-GSK3β cascade regulates Snail1 activity in breast cancer cells, Nat. Cell Biol. 8 (2006) 1398–1406, https://doi.org/10.1038/ncb1508.
[49] S. Shin, K. Jing, S. Jeong, N. Kim, K.-S. Song, J.-Y. Heo, J.-H. Park, K.-S. Seo, J. Han, J.-I. Park, G.-R. Kweon, S.-K. Park, T. Wu, B.-D. Hwang, K. Lim, The omega-3 polyunsaturated fatty acid DHA induces simultaneous apoptosis and autophagy via mitochondrial ROS-mediated Akt-mTOR signaling in prostate cancer cells expressing mutant p53, BioMed Res. Int. 2013 (2013) 568671, https://doi.org/10.1155/2013/568671.
[50] Y. Yin, C. Sui, F. Meng, P. Ma, Y. Jiang, The omega-3 polyunsaturated fatty acid docosahexaenoic acid inhibits proliferation and progression of non-small cell lung cancer cells through the reactive oxygen species-mediated inactivation of the PI3K/Akt pathway, Lipids Health Dis. 16 (2017) 87, https://doi.org/10.1186/s12944-017-0474-x.
[51] M.M. Hopkins, Z. Zhang, Z. Liu, K.E. Meier, Eicosopentaneoic acid and other free fatty acid receptor agonists inhibit lysophosphatidic acid- and epidermal growth factor-induced proliferation of human breast cancer cells, J. Clin. Med. 5 (2016) 16, https://doi.org/10.3390/jcm5020016.
[52] M. Zhang, S.F. Qiu, Activation of GPR120 promotes the metastasis of breast cancer through the PI3K/Akt/NF-κB signaling pathway, Anti Canccer Drugs 30 (2019) 260–270, https://doi.org/10.1097/CAD.0000000000000716.
[53] X. Pang, W. Fu, J. Wang, D. Kang, X. Xu, Y. Zhao, A.L. Liu, G.H. Du, Identification of estrogen receptor α antagonists from natural products via *in vitro* and *in silico* approaches, Oxid. Med. Cell. Longev. 2018 (2018) 6040149, https://doi.org/10.1155/2018/6040149.
[54] K.J. Chavez, S.V. Garimella, S. Lipkowitz, Triple negative breast cancer cell lines: one tool in the search for better treatment of triple negative breast cancer, Breast Dis. 32 (2010) 35–48, https://doi.org/10.3233/BD-2010-0307.